



Contents lists available at ScienceDirect

Optik

journal homepage: www.elsevier.de/ijleo

Compact microstrip lowpass filter with ultra-sharp roll-off and ultra-wide stopband using stepped impedance Hairpin resonator

Mohsen Hayati^{a,c,*}, Hamid Sherafat Vaziri^b, Milad Ekhteraei^b, Farzin Shama^c^a Electrical Engineering Department, Faculty of Engineering, Razi University, Kermanshah 67149, Iran^b Young Researchers and Elite Club, Kermanshah Branch, Islamic Azad University, Kermanshah, Iran^c Department of Electrical Engineering, Kermanshah Branch, Islamic Azad University, Kermanshah, Iran

ARTICLE INFO

Article history:

Received 31 January 2016

Accepted 7 March 2016

Available online xxx

Keywords:

Bended structure

Lowpass filter (LPF)

Microstrip

Ultra-sharp roll-off

Ultra-wide stopband

ABSTRACT

A novel microstrip lowpass filter (LPF) with very sharp roll-off, compact size and ultra-wide stopband is presented in this paper. The structure consists of modified stepped impedance Hairpin resonator and a circular patch as a suppressor. The proposed LPF has the cut-off frequency of 1.07 GHz. The simulation results indicated that the transition-band of the proposed LPF is 0.09 GHz from -3 to -20 dB. Maximum insertion-loss at about 80% of the passband is 0.1 dB. The proposed LPF has been designed, fabricated and measured. From the measurements, good agreements with the simulated results are obtained. Also, an ultra-wide stopband was achieved. Proposed LPF has an ultra high figure-of-merit (FOM) of 151,523, which shows its strong efficiency.

© 2016 Published by Elsevier GmbH.

1. Introduction

The most important challenge of a filter design in microwave field is that of the optimization of the device parameters [1]. Lowpass filters (LPFs) are crucial components in microwave applications, which can be used to block unwanted high frequency harmonics and to reject the spurious responses. To meet the size requirements of modern microwave communication systems, compact microwave LPFs with low insertion-loss, sharp transition-band and wide stopband width are highly desirable in RF front-end researches. In [2], a compact LPF with sharp roll-off is presented but the structure suffers from a low return-loss in the passband, low attenuation level in the stopband and complex structure because of using DGS technique. In [3], an LPF with compact size, low insertion-loss and high return-loss in the passband is presented but the filter has a gradual roll-off. In [4], an LPF with sharp roll-off and high attenuation level in stopband is presented. The weaknesses of the presented structure are its high insertion-loss (almost 2 dB) and low return-loss (near to 11 dB) in passband. In [5], a compact low-pass filter using triangular-shaped patches is presented. Although the filter has a sharp roll-off, but the stopband is narrow and the value of FOM shows its inefficiency. An LPF with extended stop-

band and compact size using M-shaped units is presented in [6]. The structure has a high suppression level in the stopband but the roll-off is not so sharp and the value of relative stopband is not so high. In [7], a compact lowpass filter with extended stopband is presented but the filter has a gradual roll-off and it also has complex structure.

In this paper, a compact lowpass filter with very sharp roll-off and ultra-wide stopband width and ultra-high FOM is presented. The presented LPF is designed, simulated and fabricated. There is an acceptable agreement between the simulation and measurement results.

2. Filter design

Fig. 1 shows the structure of conventional Hairpin resonator. The equivalent LC model of the structure and also its theoretical analysis are discussed in [8], but they are presented briefly in this paper.

As it is clear in Fig. 1, the structure consists of a high-impedance inductive line and also low-impedance coupled lines. The ABCD matrix of the inductive line and coupled lines are shown in Fig. 2.

In Fig. 2, β is the phase constant of the single transmission line, Z_{oe} and Z_{oo} are the even-mode and odd-mode impedances of the coupled lines and θ_{eff} is the arithmetic-averaged electrical length the even-mode length of the parallel coupled lines.

The equivalent LC model of the single transmission line and also parallel coupled lines are shown in Fig. 3.

* Corresponding author at: Electrical Engineering Department, Faculty of Engineering, Razi University, Kermanshah 67149, Iran. Tel.: +98 9188312041.

E-mail addresses: Mohsen.hayati@yahoo.com, hayati@razi.ac.ir (M. Hayati).

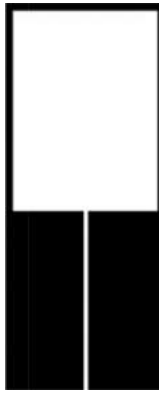


Fig. 1. Structure of the conventional Hairpin resonator.

$$\begin{aligned} \text{For } Ls, Zs: \quad [A \ B] &= \begin{bmatrix} \cos(\beta s Ls) & jZs \sin(\beta s Ls) \\ jYs \sin(\beta s Ls) & \cos(\beta s Ls) \end{bmatrix} \\ \text{For } Z_{oe}, Z_{oo}, \theta_{eff}: \quad [A \ B] &= \begin{bmatrix} \frac{Z_{oe} + Z_{oo}}{Z_{oe} - Z_{oo}} & -j \frac{2Z_{oe} Z_{oo} \cot(\theta_{eff})}{Z_{oe} - Z_{oo}} \\ j \frac{2}{(Z_{oe} - Z_{oo}) \cot(\theta_{eff})} & \frac{Z_{oe} + Z_{oo}}{Z_{oe} - Z_{oo}} \end{bmatrix} \end{aligned}$$

Fig. 2. The ABCD matrix of single transmission line and parallel coupled lines.

The value of the elements in the LC circuit model can be calculated using the ABCD matrices as below:

$$L = \frac{1}{\omega} \times Zs \times \sin\left(\frac{2\pi}{\lambda_g} l\right) \quad (1)$$

$$Cs = \frac{1}{\omega} \times \frac{1}{Zs} \times \tan\left(\frac{\pi}{\lambda_g} l\right) \quad (2)$$

$$Cc = \frac{-Im(Y21)}{\omega c} \quad (3)$$

$$Cp = \frac{Im(Y11 + Y21)}{\omega c} \quad (4)$$

In this work, the conventional Hairpin structure is modified in order to enhance the performance and also reduction of the size. Fig. 4 shows the proposed resonator. As it is clear in Fig. 4, the proposed structure is achieved by bending the low-impedance part of the conventional Hairpin resonator.

The EM-simulation results of the proposed resonator are shown in Fig. 5.

All the simulations in this paper are done using ADS software by choosing the substrate with dielectric constant of 2.22, thickness of 20 mil (0.508 mm) and loss-tangent of 0.0009.

Fig. 6 shows the LC circuit model of the designed resonator.

The values of the LC elements in Fig. 6 are shown in Table 1.

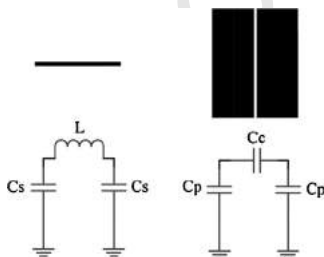


Fig. 3. The equivalent LC model of the single transmission line and parallel coupled lines.

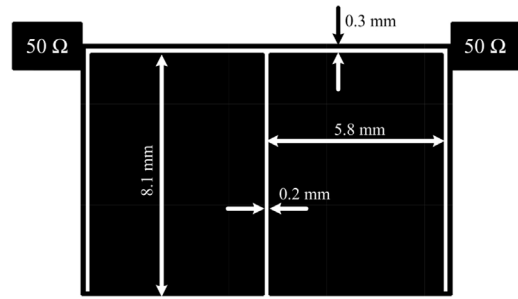


Fig. 4. Proposed modified Hairpin resonator.

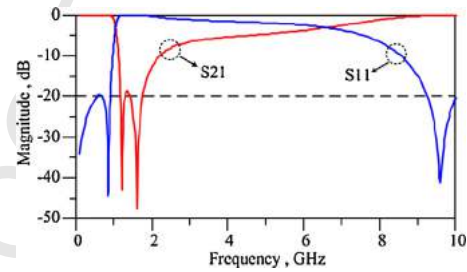


Fig. 5. EM-simulation results of the proposed resonator.

A comparison between the EM-simulation and LC circuit results of the designed resonator are shown in Fig. 7 and as it is clear, there is a good agreement between the results.

As can be seen in Fig. 5, the proposed resonator has some strong points such as: very sharp roll-off skirt, very low insertion-loss and

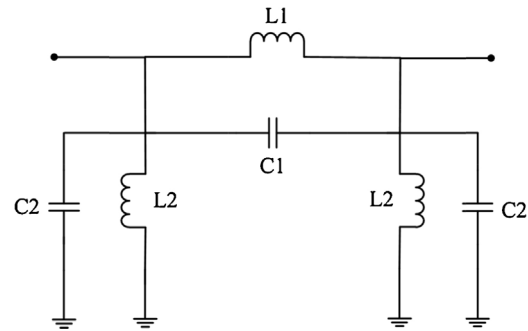


Fig. 6. LC circuit model for the designed resonator.

Table 1

The values of the LC elements.

Element	L1	L2	C1	C2
Value	9 nH	4.8 nH	4.7 pF	1.5 pF

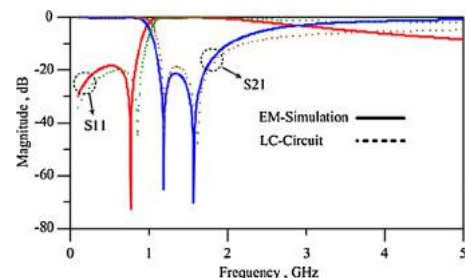


Fig. 7. Comparison between the EM-simulation and LC circuit results of the designed resonator.

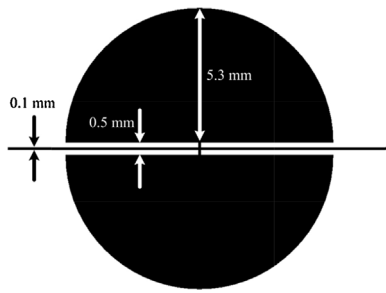


Fig. 8. Circular patch (as the suppressor).

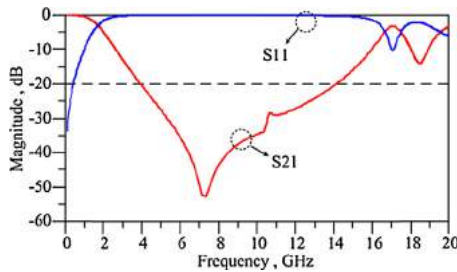


Fig. 9. Simulation results of the suppressor.

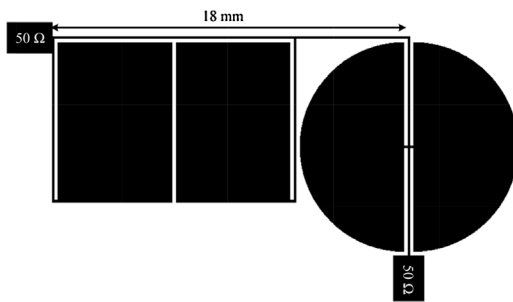


Fig. 10. Proposed LPF.

high return-loss in the passband and compact size ($<100 \text{ mm}^2$). The only weak point of the proposed resonator is the low attenuation level in the stopband. This can be solved using a proper suppressing unit. In [9], a circular patch is used as the suppressing cell which is shown in Fig. 8 and its simulation results are shown in Fig. 9.

As can be seen in Fig. 9, the employed structure has a high level of attenuation between 4 GHz and 14 GHz and so it can be used in order to increase the attenuation level in the stopband of the proposed resonator.

By adding the suppressor to the proposed resonator, the final structure will be achieved.

Fig. 10 shows the proposed LPF and the EM-simulation results are shown in Fig. 11. As it is clear in Fig. 11, the designed LPF has all the benefits of the proposed resonator and indeed, the attenuation level in the stopband is extremely increased.

The frequency response of the final topology can be determined as a Gaussian approximation. The insertion loss (in dB) approaches the Gaussian form as below [10]:

$$LA(f) = 10 \log e^{\frac{(2\pi f)^2}{(2n-1)}} \quad (5)$$

Table 2

The constant parameters for the Gaussian approximation of the insertion loss.

$a_1 = 0.5858$	$a_2 = -44.97$	$a_3 = -50.69$	$a_4 = 29.83$	$a_5 = -36.47$	$a_6 = -29.55$	$a_7 = -29.55$
$b_1 = 0.75$	$b_2 = 13.01$	$b_3 = 7.499$	$b_4 = 0.9049$	$b_5 = 1.441$	$b_6 = 3.552$	$b_7 = 0.7663$
$c_1 = 0.002148$	$c_2 = 3.192$	$c_3 = 1.845$	$c_4 = 0.491$	$c_5 = 0.4083$	$c_6 = 2.031$	$c_7 = 0.3453$

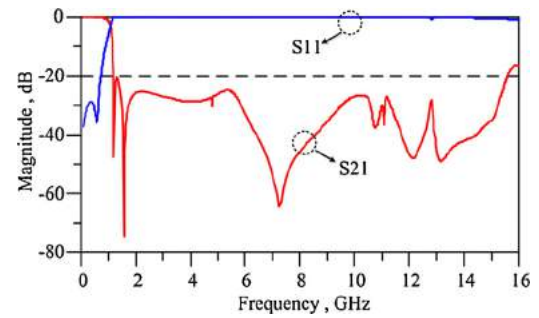


Fig. 11. EM-simulation results of the proposed LPF.

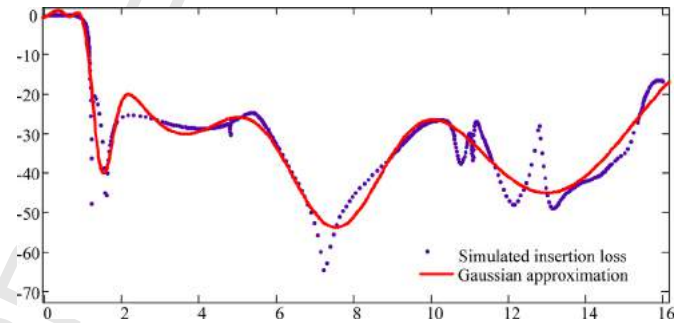


Fig. 12. The simulated insertion loss of the proposed LPF in comparison with the Gaussian approximation.

where, f is the frequency in GHz and n is order of the filter. The mentioned equation in [10] is achieved for the proposed LPF in the order of 7th as:

$$LA(f) = \left[a_1 e^{-\left(\frac{f-b_1}{c_1}\right)^2} + a_2 e^{-\left(\frac{f-b_2}{c_2}\right)^2} + a_3 e^{-\left(\frac{f-b_3}{c_3}\right)^2} + a_4 e^{-\left(\frac{f-b_4}{c_4}\right)^2} + a_5 e^{-\left(\frac{f-b_5}{c_5}\right)^2} + a_6 e^{-\left(\frac{f-b_6}{c_6}\right)^2} + a_7 e^{-\left(\frac{f-b_7}{c_7}\right)^2} \right] \text{ dB} \quad (6)$$

where, the a_i , b_i and c_i ($i=1,2,3,\dots,7$) are the constant parameters, which are determined for the -3 dB cut-off frequency at 1.07 GHz as illustrated in Table 2.

The Gaussian approximation for the insertion loss of the proposed LPF in comparison with the simulated insertion loss is depicted in Fig. 12.

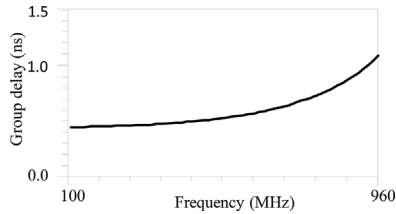
As illustrated in Fig. 12, the Gaussian approximation has an accurate adaptation in cut-off frequency, transition band and stopband bandwidth.

A high-order Gaussian filter is usually used to obtain a flat group delay over a large passband region [10]. The measured group delay of the proposed LPF is illustrated in Fig. 13. As obtained, the

Table 3

Comparison between the performance of the proposed LPF and some other related works.

REF	f_c (GHz)	ζ (dB/GHz)	RSB	I-L (dB)	R-L (dB)	SF	NCS (λ_g^2)	Resonator structure	FOM
[2]	3.14	70	1.4	–	13	1	0.0272	DGST-shaped	1200
[3]	1.2	16.9	1.38	–	17	1.5	0.0095	Stepped impedance	3682
[4]	1.65	57.8	1.61	–	–	3.5	0.0120	Coupled rhombic	27,142
[5]	5.55	84	0.67	0.7	20	1.5	0.0857	Triangle patch	985
[6]	1.8	45.12	1.33	0.25	20	4	0.0200	M-shaped	12,000
[7]	1	23.6	1.76	0.4	7	1.5	0.0101	Triangular and radial	6169
[11]	1.6	52.8	1.53	0.3	17	2	0.0091	Hairpin	17,755
[12]	2.97	84.69	1.51	0.06	18.7	2	0.0223	Hexangular	11,625
[13]	1.3	143	1.76	–	12	2	0.0109	Stepped impedance	46,074
LPF1 [14]	1.71	100	1.71	0.1	18	1.6	0.0200	Tapered	13,680
LPF2 [14]	1.49	44.7	1.85	0.98	13	2	0.0200	Tapered	8270
This work	1.07	264.28	1.72	0.08	18	2	0.0060	Hairpin	151,523

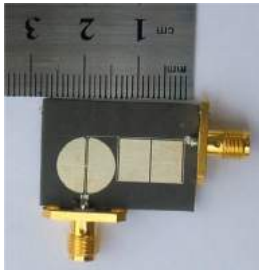
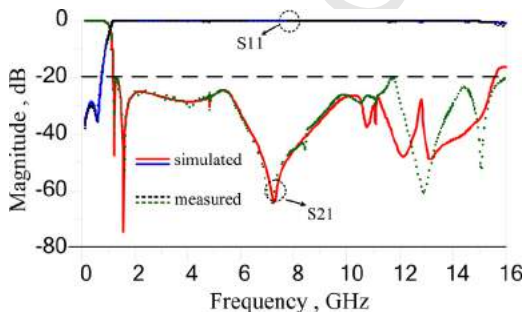
**Fig. 13.** The measured groups delay of the proposed LPF in the passband.

maximum variation of the proposed filter in this region is only 0.5 ns, which shows a good performance.

3. Fabrication and measurement

The proposed LPF is fabricated on RT/Duroid 5880 substrate using microelectronic technology with dielectric constant of 2.22, height of 20 mil (0.508 mm) and loss-tangent of 0.0009. The fabricated filter is measured using the Agilent network analyzer N5230A.

Fig. 14 shows the photograph of the fabricated LPF and a comparison between the simulation and fabrication results is shown in Fig. 15.

**Fig. 14.** Photograph of the fabricated LPF.**Fig. 15.** Comparison between the simulation and the measured results of the proposed LPF.

The measured results show that the proposed LPF has cut-off frequency at 1.07 GHz. It also has an ultra-wide stopband width of 14.4 GHz (from 1.18 GHz to 15.58 GHz for the suppression level more than -20 dB). The value of insertion-loss in passband is lower than 0.08 dB and the return-loss in the pass band is more than 18 dB. The proposed LPF has an ultra sharp roll-off rate of 264.28 dB/GHz. The size of the proposed LPF is $0.05\lambda_g \times 0.11\lambda_g$ where, λ_g is the guided wave length at the cut-off frequency. Considering all the above characteristics, the proposed LPF has an ultra-high FOM of $151,523$ which shows its strong efficiency.

Table 3 shows a comparison between the performance of the proposed structure and some other related works. In this table, the definition of the roll-off rate is:

$$\xi = \frac{\alpha_{\max} - \alpha_{\min}}{f_s - f_c} \text{ (dB/GHz)} \quad (5)$$

In this equation, α_{\max} and α_{\min} are located at the -20 dB attenuation point and the -3 dB attenuation point, respectively; f_s and f_c are the -20 dB stopband frequency and the -3 dB cut-off frequency, respectively. The definition of the relative stopband bandwidth (RSB) is:

$$\text{RSB} = \frac{\text{Stopband bandwidth}}{\text{Stopband center frequency}} \quad (6)$$

The suppression factor (SF) is depended on stopband bandwidth. For example, if the rejection level in the stopband is calculated under 20 dB, then the SF is considered to be 2 . The normalized circuit size (NCS) is calculated from following relation:

$$\text{NCS} = \frac{\text{physical size (length} \times \text{width)}}{\lambda_g^2} \quad (7)$$

In this relation, λ_g is defined as the guided wavelength at -3 dB cut-off frequency. The architecture factor can be known as the circuit complexity factor, which is fixed as 1 and 2 , for a $2D$ and $3D$ structure, respectively. Finally, the figure-of-merit (FOM) is the overall index of a lowpass filter and can be calculated from below relation as:

$$\text{FOM} = \frac{\text{RSB} \times \xi \times \text{SF}}{\text{AF} \times \text{NCS}} \quad (8)$$

As it is clear in Table 3, the proposed LPF has an excellent performance in comparison with other related works.

4. Conclusion

A novel LPF using modified stepped impedance Hairpin resonator is presented in this paper. The proposed LPF has -3 dB cut-off frequency at 1.07 GHz. The design procedure started with designing the main resonator and then, suitable suppressor were added to the structure to improve its performance. At the end, in order to judge about the performance of the proposed LPF, its characteristics were compared with some other

related works. The comparison shows that, the proposed LPF had better performance in comparison with other works and so it can be used to answer the demands in modern communication systems.

References

- [1] I.A. Dovbysh, V.V. Tyurnev, Intelligence method for optimizing a microstrip filter based on folded dual-mode resonators, *J. Commun. Technol. Electron.* 54 (11) (2009) 1269–1273.
- [2] A. Faraghi, M. Ojaroudi, N. Ghadimi, Compact microstrip low-pass filter with sharp selection characteristics using triple novel defected structures for UWB applications, *Microw. Opt. Technol. Lett.* 56 (4) (2014) 1007–1010.
- [3] X. Chen, et al., Compact lowpass filter with wide stopband bandwidth, *Microw. Opt. Technol. Lett.* 57 (2) (2015) 367–371.
- [4] B. Zhang, S. Li, J. Huang, Compact lowpass filter with wide stopband using coupled rhombic stubs, *Electron. Lett.* 51 (3) (2015) 264–266.
- [5] P.M. Raphika, P. Abdulla, P.M. Jasmine, Compact lowpass filter with a sharp roll-off using patch resonators, *Microw. Opt. Technol. Lett.* 56 (11) (2014) 2534–2536.
- [6] Z. Du, et al., Compact lowpass filter with high suppression level and wide stopband using stepped impedance M-shape units, *Microw. Opt. Technol. Lett.* 56 (12) (2014) 2947–2950.
- [7] J. Wang, H. Cui, G. Zhang, Design of compact microstrip lowpass filter with ultra-wide stopband, *Electron. Lett.* 48 (14) (2012) 854–856.
- [8] M.H. Yang, et al., Wide-stopband and miniaturized lowpass filters using sirs-loaded hairpin resonators, *J. Electromagn. Waves Appl.* 23 (17–18) (2009) 2385–2396.
- [9] M. Hayati, et al., Compact microstrip lowpass filter with very sharp roll-off and ultra-high figure-of-merit for wireless applications, *J. Electromagn. Waves Appl.* 29 (11) (2015) 1508–1522.
- [10] J.-S.G. Hong, M.J. Lancaster, *Microstrip Filters for RF/Microwave Applications*, 167, John Wiley & Sons, 2004.
- [11] S. Liu, J. Xu, X. Zhitao, Compact lowpass filter with wide stopband using stepped impedance hairpin units, *Electron. Lett.* 51 (1) (2014) 67–69.
- [12] M. Hayati, et al., Design of microstrip lowpass filter with wide stopband and sharp roll-off using hexangular shaped resonator, *Electron. Lett.* 51 (1) (2014) 69–71.
- [13] K. Dehghani, et al., Design of lowpass filter using novel stepped impedance resonator, *Electron. Lett.* 50 (1) (2014) 37–39.
- [14] S. Majidifar, High performance microstrip LPFs using dual taper loaded resonator, *Optik Int. J. Light Electron Opt.* 127 (6) (2016) 3484–3488.